in the simple model we have used for the cooling process. Furthermore, the prediction $\beta/\xi_0 = (\tau_Q/\tau_0)^{1/4}$ from the Zurek model is only qualitative.

This close agreement, however, does confirm that a fast cooling through the superfluid transition indeed creates a residual density of vortices as foreseen in Zurek's model of the Kibble mechanism. That the observed vortices are further spaced than the theory suggests may simply be a reflection of the approximations made both in deducing the value from the data and estimating the equivalent number from Zurek's expression. Why the observed separation, β/ξ_0, is apparently independent of pressure is not clear at present. Finally, if indeed analogous topological objects have once existed or even survive in the Universe, then we have taken the first tentative steps with superfluid ^{3}He towards the quantitative modelling of their formation. □

Received 15 January; accepted by 4 June 1996.

1. Kibble, T. W. B. *J. Phys.* A**9**, 1387–1398 (1976).
2. Hendry, P. C., Lawson, N. S., Lee, R. A. M., McClintock, P. V. E. & Willians, C. H. D. *Nature* **368**, 315–317 (1994).
3. Zurek, W. H. *Nature* **317**, 505–508 (1985).
4. Volovik, G. E. *Exotic Properties of Superfluid ^{3}He* (World Scientific, Singapore, 1992).
5. Bradley, D. I. *et al. Phys. Rev. Lett.* **75**, 1887–1891 (1995).
6. Chuang, I., Durrer, R., Turok, N. & Yurke, B. *Science* **251**, 1336–1342 (1991).
7. Ruutu, V. M. H. *et al. Nature* **382**, 334–336 (1986).
8. Fisher, S. N., Guénault, A. M., Kennedy, C. J. & Pickett, G. R. *Phys. Rev. Lett.* **69**, 1073–1076 (1992).
9. Adams, J. S. *et al. Phys. Lett.* B**341**, 431–434 (1995).

ACKNOWLEDGEMENTS. We thank G. Volovik for discussions, and J.-L. Bret, J. Chaussy and L. Puech for their assistance with the electronics and computer programming. This work was supported in part by Etat/DRET.

CORRESPONDENCE should be addressed to Y.M.B. (e-mail: bunkov@labs.polycnrs-gre.fr).

Vortex formation in neutron-irradiated superfluid ^{3}He as an analogue of cosmological defect formation

V. M. H. Ruutu*, V. B. Eltsov*†, A. J. Gill‡§, T. W. B. Kibble‡, M. Krusius*, Yu. G. Makhlin*||, B. Plaçais¶, G. E. Volovik*|| & Wen Xu*

* Low Temperature Laboratory, Helsinki University of Technology, 02150 Espoo, Finland
† Kapitza Institute for Physical Problems, 117334 Moscow, Russia
‡ Blackett Laboratory, Imperial College, London SW7 2BZ, UK
§ T-6 Theoretical Division, Los Alamos National Laboratory, Los Alamos, New Mexico 87545, USA
|| Landau Institute for Theoretical Physics, 117334 Moscow, Russia
¶ Laboratoire de Physique de la Matière Condensée de l'Ecole Normale Supérieure, CNRS URA 1437, F-75231 Paris Cedex 05, France

TOPOLOGICAL defects formed during a rapid symmetry-breaking phase transition in the early Universe[1,2] could be responsible for seeding large-scale structure, for the anisotropy of the microwave background radiation, and for the predominance of matter over antimatter[3,4]. The theory describing this cosmological phase transition is formally analogous to that describing the transition to the superfluid state in liquid ^{3}He, so that in principle the process of cosmological defect formation can be modelled in the laboratory. Here we report the results of an experiment in which the 'primordial fireball' is mimicked using a neutron-induced nuclear reaction (n + ^{3}He → p + ^{3}He + 0.76 MeV) to heat small regions of superfluid ^{3}He above the superfluid transition temperature. These bubbles of normal liquid cool extremely rapidly, and we find that their transition back to the superfluid state is accompanied by the formation of a random network of vortices (the superfluid analogue of cosmic strings). We monitor the evolution of this defect state by rotating the superfluid sample, allowing vortices to escape from the network and thus be probed individually. Our results provide clear confirmation of the idea that topological defects form at a rapid second-order phase transition, and give quantitative support to the Kibble–Zurek mechanism[5,6] of cosmological defect formation.

Laboratory experiments intended to test different theories of cosmological defect formation have recently been conducted in liquid crystals[7,8] and superfluid ^{4}He (ref. 9). Use of the superfluid phases of liquid ^{3}He allows further progress in these Big Bang simulations. ^{3}He has several advantages over other systems. Many direct parallels and formal analogies connect superfluid ^{3}He theory with the field theories that are used to describe the physical vacuum, gauge fields and fermionic elementary particles[10]. Superfluid ^{3}He exhibits a variety of phase transitions and topological defects which can be detected with NMR methods with single-defect sensitivity[11]. Different modern models of defect-mediated baryogenesis[3,4,12] can be simulated by the interaction of the ^{3}He defects, vortices and domain walls, with fermionic quasiparticles. Of particular relevance to our rapid-quench experiment is the fact that liquid ^{3}He can be efficiently locally heated with thermal neutrons (Fig. 1).

The neutrons are produced with a paraffin-moderated Am–Be source of 10 mCi activity. They are then incident upon the ^{3}He sample container. At the minimum distance of 22 cm between

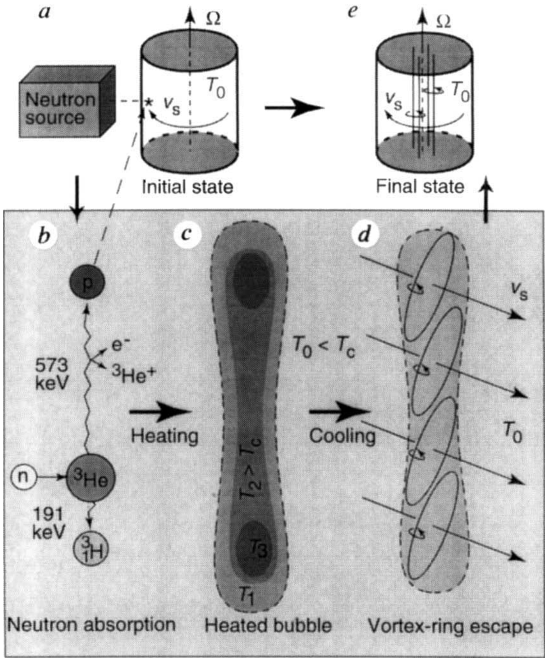

FIG. 1 Principle of the experiment and of vortex formation during neutron irradiation: *a*, Superfluid ^{3}He-B contained in a cylinder, which rotates at constant angular velocity Ω, is exposed to neutron radiation. *b*, In a neutron-absorption event, a proton and a tritium nucleus are formed which fly apart in opposite directions. Their kinetic energies are used up in ionization reactions of ^{3}He atoms. *c*, The ionized particles recombine, generating heat in the form of quasiparticle excitations which corresponds to a substantial part of the total reaction energy. A cigar-shaped hot region of liquid is formed where the temperature rises above T_c. *d*, The hot bubble cools rapidly towards the bulk liquid temperature T_0. While passing through the superfluid transition at T_c a tangled network of vortex lines is formed. Vortex loops which exceed a critical size start to expand in the superfluid flow created by the rotation of the container whereas smaller loops contract and annihilate. *e*, An expanding vortex ring ultimately intersects the walls of the container and gives rise to one rectilinear vortex line. The vortex lines accumulate in the centre of the rotating container where they are counted with NMR.

source and sample, $v \approx 20$ neutrons min^{-1} are absorbed by the ^{3}He liquid. For thermal neutrons the mean free path is 0.1 mm in liquid ^{3}He, and thus all absorption reactions occur close to the walls of the cylindrical container which has radius $R = 2.5$ mm. Because the incident thermal neutron has low momentum, the 573-keV proton and 191-keV tritium nucleus fly apart in opposite directions, producing ionization tracks that are 70 and 10 μm long, respectively. The subsequent charge recombination yields a heated region of the normal liquid phase which, for simplicity, we here assume to be of a spherically symmetric shape[13].

The bubble of normal fluid cools by the diffusion of quasiparticle excitations out into the surrounding superfluid with a diffusion constant $D \approx v_F l$ where v_F is their Fermi velocity and l the mean free path. The difference from the surrounding bulk temperature T_0 as a function of the radial distance r from the centre of the bubble is given by $T(r,t) - T_0 \approx E_0 \exp(-r^2/4Dt)/(C_v(4\pi Dt)^{3/2})$ where E_0 is the energy deposited by the neutron as heat and C_v is the specific heat. The maximum value of the bubble radius R_b, with fluid in the normal phase above the superfluid transition temperature $T_c \approx 2$ mK, is given for $T(r) > T_c$ by

$$R_b \approx (E_0/C_v T_c)^{1/3}(1 - T_0/T_c)^{-1/3} \quad (1)$$

which is typically of the order of 10 μm. The bubble cools and shrinks away rapidly with the characteristic time $\tau_Q \approx R_b^2/D \approx 10^{-6}$ s. The rapid superfluid phase transition leads to the formation of a random network of vortices. The fate of vorticity depends on the bias field, the external superfluid velocity $v_s = \Omega R$, created by rotating the container at an angular velocity Ω. If the radius of the vortex loop exceeds the value $r_0(v_s) = (\kappa/4\pi v_s)\ln r_0/\xi$, where $\kappa = \pi\hbar/m_3$ is the circulation quantum and $\xi = \xi_0(1 - T/T_c)^{-1/2}$ is the superfluid coherence length, the loop expands. An expanding vortex ring eventually results in a rectilinear vortex line which is pulled to the centre of the container. If several vortex lines are formed they accumulate in a central vortex bundle[11].

The number of the vortex lines is monitored with NMR. In Fig. 2 inset two NMR absorption records are shown, starting from the moment when the neutron source is placed in position. The absorption events, which lead to vortex formation, are visible as distinct steps. The step height gives the number of vortex lines created per event, if the neutron source is sufficiently far from the sample and the absorption events are well separated in time. The number of vortex lines created per unit time increases rapidly with increasing v_s (Fig. 2). The extrapolation to zero gives the threshold value v_{cn} plotted in Fig. 3 as a function of T_0 for different pressures. This v_{cn} is much smaller and has a different dependence on T_0 than the critical velocity v_c at which a vortex is formed in the absence of neutrons in the B phase of superfluid ^{3}He (^{3}He-B)[11].

According to ref. 2, the topological defects are created during the symmetry-breaking transition when the order parameter begins to fall from the false ground state into the true degenerate ground states which form independently in regions which are not causally connected. The different regions grow in size, and ultimately the order parameter fills all space but with a multitude of defects. The important notion in this theory is the initial density of defects, that is, the defect density at the moment when the defects can be distinguished from the background fluctuations of the order parameter. In the original Kibble model[2] this was identified with the moment when the system cools below the Ginzburg temperature T_G above which the thermal fluctuations prevail. This implies that the initial distance between the vortices is the coherence length at T_G, that is, $\xi(T_G) = \xi_0/\sqrt{1 - (T_G/T_c)}$. In superfluid ^{3}He the critical fluctuation region is extremely narrow, $1 - (T_G/T_c) \approx (a/\xi_0)^4$, because the zero temperature coherence length $\xi_0 \approx 0.1$ μm is two orders of magnitude larger than the interatomic spacing a (ref. 14). As a result $\xi(T_G) \approx \xi_0(\xi_0/a)^2$ exceeds the bubble size R_b, which means that no vortices can be created in this model.

In an alternative theory put forward by Zurek[5,6], the vortices are formed at the moment when the coherence length becomes comparable with the causal horizon. For ^{3}He this occurs at the time $\sqrt{\tau_Q \tau_0}$ after the transition, where $\tau_0 = \xi_0/v_F$. The value of the coherence length ξ at that instant, $\xi_0(\tau_Q/\tau_0)^{1/4}$, gives the initial distance between the defects, of the order of 1 μm in our case. This is well within R_b, in agreement with our experiment.

The later evolution of the vortex network leads to a gradual increase of the intervortex distance $\tilde{\xi}(t)$, while the network structure remains scale-invariant[3,4]. For a homogeneous system the number of loops $n(l)$ per unit length and unit volume with line lengths $l > \tilde{\xi}$ is given[15] by $n(l) = C\tilde{\xi}^{-3/2} l^{-5/2}$ where $C \approx 0.4$. For our case of finite bubble volume, where all vortices form closed loops, our numerical simulation gives the same distribution law but with slightly different $C \approx 0.3$. For the average straight-line dimension $\mathscr{D}$ of a loop we find $\mathscr{D} = \beta(l\tilde{\xi})^{1/2}$ with $\beta \approx 1$. The loop size distribution in terms of $\mathscr{D}$ is $n(\mathscr{D})\,d\mathscr{D} \approx 2C\,d\mathscr{D}/\mathscr{D}^4$, and does not depend on the distance between vortices. The evolution of the network leads to an increasing lower cut-off of the distribution, $\mathscr{D}_{min} = \alpha\tilde{\xi}(t)$, where α is of the order of unity. The upper cut-off is the diameter of the bubble $\mathscr{D}_{max} = 2R_b$.

When the average radius of curvature, determined by $\tilde{\xi}$, exceeds $r_0(v_s)$ the vortices start to escape from the bubble. The number of vortices, $\mathscr{N}(v_s)$, created per neutron is thus the number of loops with $\alpha r_0(v_s) < \mathscr{D} < 2R_b$ in the bubble volume V_b:

$$\mathscr{N}(v_s) = V_b \int_{\alpha r_0(v_s)}^{2R_b} d\mathscr{D}\, n(\mathscr{D}) = \frac{\pi C}{9}\left[\left(\frac{2R_b}{\alpha r_0(v_s)}\right)^3 - 1\right] \quad (2)$$

The critical velocity v_{cn} is determined by the requirement $\mathscr{N}(v_{cn}) = 0$, which gives $v_{cn} = (\kappa\alpha/8\pi R_b)\ln(R_b/\xi)$. Our numerical simulation suggests $\alpha \approx 1$. Thus v_{cn} is inversely proportional to R_b

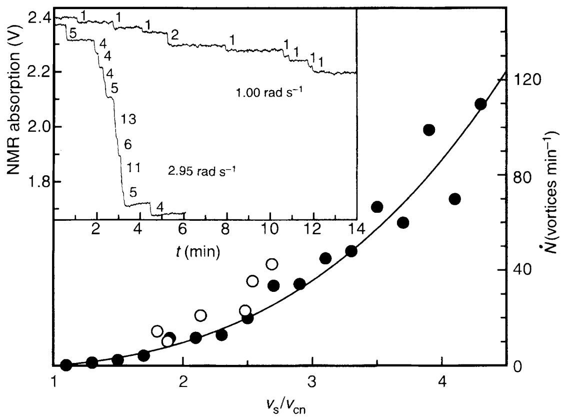

FIG. 2 Formation of vortices during neutron irradiation. Inset, change in NMR absorption as a function of running time t at high and low rotation velocity. The neutron source is turned on at $t = 0$. Each step corresponds to one neutron absorption event. The height of the step gives the number of vortex lines created and is denoted by the adjacent number. The high-velocity trace is recorded with the neutron source at a 2.8 times larger distance from the ^{3}He-B sample. The bulk liquid temperature is $T_0 = 0.96\,T_c$. Main figure, the rate $\dot{N}$ at which vortex lines are created during neutron irradiation, plotted as a function of the normalized superfluid velocity v_s/v_{cn}. Below the critical threshold at v_{cn} the rate vanishes, while above the threshold the rate follows the fitted cubic dependence $\dot{N} = \gamma[(v_s/v_{cn})^3 - 1]$, with $\gamma = (1.37 \pm 0.06)$ vortex lines per min, shown by the solid line. The rate of vortex formation is the number of vortices per neutron $\mathscr{N}(v_s)$ multiplied by the neutron flux v: $\dot{N} = v\mathscr{N}(v_s)$. The theoretical estimate for $\mathscr{N}(v_s)$ from equation (3) with $v \approx 20$ neutrons min^{-1} gives $\gamma = v\pi C/9 \approx 2$, which is in order-of-magnitude agreement with the experiment. The filled circles show data measured at a bulk liquid temperature $T_0 = 0.96\,T_c$; the open circles, data measured at $0.90\,T_c$. Both sets of data fall on the same cubic dependence, although v_{cn} differs by 50% (Fig. 3). The cubic dependence on the superflow velocity is ultimately interrupted by the spontaneous critical velocity $v_c(T_0, P)$, which is the maximum possible superflow velocity and here at $0.96\,T_c$ about $6.5\,v_{cn}$. The liquid pressure $P = 18.0$ bar and the magnetic field $B = 11.8$ mT are the same as in the inset.

and according to equation (1) has the temperature dependence $v_{cn} \propto (1 - T_0/T_c)^{1/3}$, in agreement with the measurements in Fig. 3. In terms of v_{cn} one obtains the universal curve

$$\mathcal{N}(v_s/v_{cn}) = \frac{\pi C}{9}\left[\left(\frac{v_s}{v_{cn}}\right)^3 - 1\right] \quad (3)$$

Equation (3) reproduces the observed cubic velocity dependence and gives the correct order of magnitude estimate of $\mathcal{N}(v_s)$, as seen in Fig. 2. It also carries the same universality feature as the measured results in Fig. 3: the ambient measuring conditions depend on what values are chosen of the temperature T_0, pressure P, and magnetic field B, but in the results for $\mathcal{N}(v_s)$ all this dependence is contained in the single parameter v_{cn}.

The experiment demonstrates that vortices are created within bulk liquid ^{3}He during a rapid quench to the superfluid state. The measured number of vortices created as a function of velocity is consistent with the Vachaspati–Vilenkin scaling law[15] discussed for cosmic strings. This is a strong argument in favour of the Kibble–Zurek mechanism of defect formation. The external flow mainly plays the role of the bias field which allows vortices to escape, to expand and finally to reach a stable state in the rotating container so that they can be detected one-by-one. With increasing superfluid velocity v_s, smaller loops, which represent an earlier stage in the evolution of the network, are extracted. We expect that when we reach the smallest possible size of loops, which is limited by the initial interdefect distance, the cubic scaling law will be violated. At the moment, the smallest size of the loops extracted at the highest rotation velocity is above, but close to, the limit which follows from the Zurek model, but is several orders of magnitude smaller than suggested by the original Kibble theory. This supports the Zurek modification of the Kibble mechanism. We are planning to study the Kibble mechanism for formation of other types of defects in superfluid ^{3}He, such as half-quantum vortices (Alice strings) and domain walls. Superfluid ^{3}He is also the only condensed-matter system where one can try to simulate the processes of interaction of defects with fermions that lead to the baryon asymmetry.

The Kibble–Zurek mechanism, based on a simple physical picture, gives a good quantitative fit to our measurements. Vortex formation in neutron-irradiated superfluid ^{3}He now provides the most stringent confirmation of the formation of topological defects at a rapid second-order phase transition, and allows quantitative comparison with the estimated loop size distribution. This gives confidence in applications of similar ideas to the early Universe, where topological defects remain a viable explanation for large-scale structure formation and the microwave background anisotropy. Detailed predictions, for example of the intensity of gravitational radiation emitted by oscillating cosmic strings, are strongly dependent on the initial density of strings at formation. □

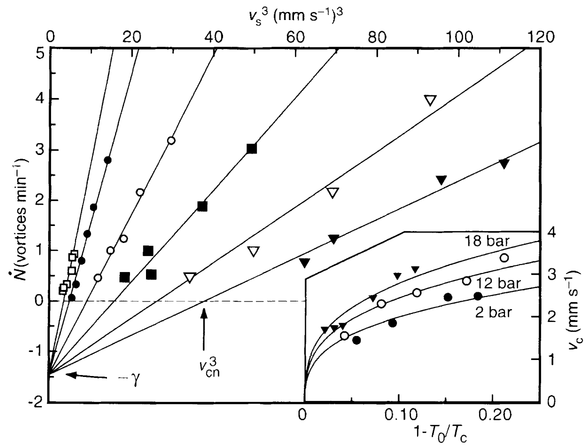

FIG. 3 Inset, critical superflow velocities as a function of the normalized bulk liquid temperature $1 - T_0/T_c$ and pressure P of the liquid ^{3}He-B sample in a magnetic field of $B = 11.8$ mT. Solid lines, critical value of superflow velocity $v_{cn} \propto (1 - T_0/T_c)^{1/3}$ at which vortex creation starts in the presence of the neutron source. Main figure, the rate $\dot{N}$ at which vortex lines are created during neutron irradiation, plotted as a function of v_s^3, demonstrating the scale-invariance of the vortex-formation law in different ambient conditions: $P = 2$ bar, $T_0 = 0.95T_c$, $B = 11.8$ mT (empty squares); $P = 12$ bar, $T_0 = 0.96T_c$, $B = 11.8$ mT (filled circles); $P = 18$ bar, $T_0 = 0.97T_c$, $B = 16$ mT (empty circles); $P = 18$ bar, $T_0 = 0.97T_c$, $B = 28$ mT (filled squares); $P = 18$ bar, $T_0 = 0.90T_c$, $B = 28$ mT (empty triangles); $P = 18$ bar, $T_0 = 0.91T_c$, $B = 60$ mT (filled triangles). In agreement with equation (3), the dependence on temperature T_0, pressure P, and magnetic field B is contained in the critical velocity v_{cn}. The intercept of the fitted lines with the horizontal axis yields v_{cn}^3. The common intercept with the vertical axis, $\gamma = (1.46 \pm 0.12)$ vortex lines per min, defines the numerical prefactor in equation (3).

Received 21 December 1995; accepted 4 June 1996.

1. Zeldovich, Ya. B., Kobzarev, I. Yu. & Okun, L. B. *Zh. éksp. teor. Fiz.* **67**, 3–11 (1974); (*JETP* **40**, 1–5 (1974).).
2. Kibble, T. W. B. *J. Phys.* A**9**, 1387–1398 (1976).
3. Vilenkin, A. & Shellard, E. P. S. *Cosmic Strings and Other Topological Defects* (Cambridge Univ. Press, 1994).
4. Hindmarsh, M. B. & Kibble, T. W. B. *Rep. Prog. Phys.* **58**, 477–562 (1995).
5. Zurek, W. H. *Nature* **317**, 505–508 (1985).
6. Zurek, W. H. *Los Alamos preprint LA-UR-95-2269 (1995); Phys. Rep.* (in the press); *Acta physica polonica* B**24**, 1301–1311 (1993).
7. Chuang, I., Durrer, R., Turok, N. & Yurke, B. *Science* **251**, 1336–1342 (1991).
8. Bowick, M. J., Chander, L., Schiff, E. A. & Srivastava, A. M. *Science* **263**, 943–945 (1994).
9. Hendry, P. C., Lawson, N. S., Lee, R. A. M., McClintock, P. V. E. & Williams, C. D. H. *Nature* **368**, 315–317 (1994).
10. Volovik, G. E. & Vachaspati, T. *Int. J. mod. Phys.* B**10**, 471–521 (1996).
11. Parts, Ü *et al. Europhys. Lett.* **31**, 449–454 (1995).
12. Turok, N. in *Formation and Interaction of Topological Defects* (eds Davis, A. C. & Brandenberger, R.) 283–301 (Plenum, New York, 1995).
13. Schiffer, P. & Osheroff, D. D. *Rev. mod. Phys.* **67**, 491–501 (1995).
14. Vollhardt, D. & Wölfle, P. *The Superfluid Phases of ^{3}He* (Taylor & Francis, London, 1990).
15. Vachaspati, T. & Vilenkin, A. *Phys. Rev.* D**30**, 2036–2045 (1984).

ACKNOWLEDGEMENTS. This collaboration was carried out under the EU Human Capital and Mobility programme. A.J.G., T.W.B.K. and B.P. thank the Low Temperature Laboratory for support and hospitality.

CORRESPONDENCE should be addressed to T.W.B.K. (e-mail: kibble@ic.ac.uk).

An explanation for the central stress minimum in sand piles

J. P. Wittmer*, P. Claudin†, M. E. Cates* & J.-P. Bouchaud‡

* Department of Physics and Astronomy, University of Edinburgh, JCMB King's Buildings, Mayfield Road, Edinburgh EH9 3JZ, UK
† Cavendish Laboratory, Madingley Road, Cambridge CB3 0HE, UK
‡ Service de Physique de l'Etat Condensé, CEA Ormes des Merisiers, 91191 Gif-sur-Yvette, Cedex France

A KEY component of a continuum-mechanical description of a sand pile (viewed as an assembly of hard particles in frictional contact) is the requirement of stress continuity—the forces acting on a small element of material must balance. But an additional physical postulate is required to close the equations. Standard continuum approaches postulate that the material is everywhere just at the point of slip failure[1,2]. But these approaches have been unable to explain a startling experimental observation[3]—that the weight exerted by a conical sand pile on a surface has a minimum, not a maximum, below the apex. Here we propose a new closure, which embodies an intuitive model of arching[4,5] within a fully consistent continuum theory. Our assumption is that the principal stress axes have a fixed angle of inclination to the vertical. In two dimensions, this is sufficient to close the equations. In three dimensions, a second closure